

# Entropic Interactions in Suspensions of Semi-flexible Rods: Short-Range Effects of Flexibility

A. W. C. Lau, Keng-Hui Lin, and A. G. Yodanis

Department of Physics and Astronomy, University of Pennsylvania, Philadelphia, PA 19104  
(Dated: March 22, 2024)

We compute the entropic interactions between two colloidal spheres immersed in a dilute suspension of semi-flexible rods. Our model treats the semi-flexible rod as a bent rod at a fixed angle, set by the rod contour and persistence lengths. The entropic forces arising from this additional rotational degree of freedom are captured quantitatively by the model, and account for observations at short range in a recent experiment. Global fits to the interaction potential data suggest the persistence length of fd-virus is about two to three times smaller than the commonly used value of  $2.2 \mu\text{m}$ .

PACS numbers: 82.70.Dd, 05.40.-a, 87.15.La

Colloidal dispersions exhibit a fascinating range of equilibrium and non-equilibrium structures, and they have an important impact on our daily lives [1]. The interactions between suspension constituents determine the stability of the dispersion against coagulation, and the phase behavior of the colloid. Quantitative models and measurements of these interactions test our basic understanding about these systems, and enable experiments to better control suspension behaviors and properties. In this paper we focus on a particular class of entropic interaction, exploring the forces between spheres in a suspension of rodlike particles. This system class has produced a variety of interesting phases [2, 3, 4], and has stimulated several theoretical models [5, 6, 7, 8, 9] and a measurement [10] of the rod-induced depletion interaction.

The depletion attraction between two spheres immersed in a dilute suspension of thin rods of length,  $L_c$ , was first considered by Asakura and Oosawa [11]. Their most important physical insight was that rods in suspension gain both translational and rotational entropy when the sphere surfaces come within  $L_c$  of one another. Subsequent theories computed the attraction more accurately within the Derjaguin approximation [6, 7] and beyond [5]. However, in many practical scenarios the rods are not rigid, and current theories do not account for the flexibility of the rods. Indeed, flexibility effects can be important as evidenced by a recent interaction measurement [10] of micron diameter spheres in suspensions of fd-virus; in this case systematic deviations between experiment and "rigid-rod" theories were found at short-range, and were suggested to arise as a result of the flexibility of the fd-virus. Flexible or bent rods have an additional degree of freedom: the rotation about their central axis. As the spheres get closer, this degree of freedom is depleted, the system entropy increases, and the sphere interactions become even more attractive.

A quantitative model for this observation is still lacking, and indeed a complete theory of semi-flexible rods near surfaces remains a difficult task. In this paper, we introduce a simple model to compute the depletion potential between two spheres in a dilute solution of semi-flexible rods. We use the model to quantitatively explain the experiments of Ref. [10]. The model accounts for

the entropic effects of flexibility at short-range, and provides an accurate fit of the measured interaction potentials. The model also provides a means to extract the persistence length  $\ell_p$  and the contour length  $L_c$  of the suspended semi-flexible rods from interaction potential data. Global fitting of the data suggests that the persistence length of fd-virus is two to three times smaller than the commonly used value of  $2.2 \mu\text{m}$  [12].

Our model relies on the assumption that if the rods are sufficiently stiff, they may be accurately approximated by two rods of length  $L = L_c/2$ , attached together at a fixed angle  $2\alpha$ , as shown in Fig. 1. The angle  $\alpha$  may be estimated by  $\alpha = \cos^{-1}(R/L_c)$ , where  $R = \langle r^2 \rangle^{1/2}$  is the average end-to-end distance.  $R$  is related to  $\ell_p$  and  $L_c$  by [13]

$$\langle r^2 \rangle = 2L_c\ell_p + 2\ell_p^2 e^{-L_c/\ell_p} - 1 : \quad (1)$$

This approach simplifies the problem, while still capturing the essential physics. In particular, we show that the part of the depletion potential associated with new rotational degrees of freedom is short ranged, i.e. of order

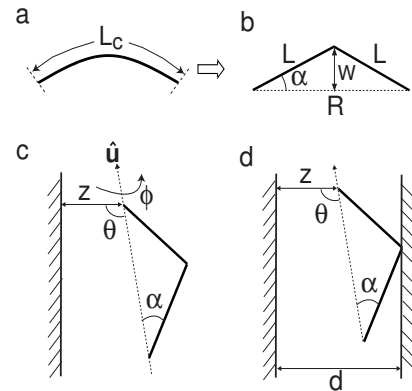


FIG. 1: (a) Typical configurations of a semi-flexible rod whose contour length  $L_c$  is comparable to the persistence length  $\ell_p$ . (b) Our approximation of semi-flexible rod in (a); two stiff rods of length  $L$  attached at a fixed angle. (c) A bent rod near a wall and (d) confined between two walls.

the bent rod width,  $W = L \sin \alpha$ . Importantly, when  $W$  is significantly less than the particle diameter, the rotational part of the depletion interaction can be treated within the Derjaguin approximation [1].

In the presence of repulsive walls (see Fig. 1), the rotational degrees of freedom of a bent rod are restricted. Consider a bent rod with one end displaced by  $z$  from the wall and with orientation  $(\hat{u}; \hat{v})$ . The probability of finding a rod in such a configuration is given by the Boltzmann factor:  $f(r; \hat{u}; \hat{v}) / \exp[-U_b(r; \hat{u}; \hat{v})]$ , where  $\beta = 1/k_B T$ ,  $k_B$  is the Boltzmann constant, and  $T$  is the temperature. The hard wall potential  $U_b$  is infinite if any part of the rod touches the wall and is otherwise zero. We consider the case where the concentration of the rods is sufficiently low so that the thermodynamics are well characterized by the Grand potential of an ideal gas of rods

$$\Omega = -N k_B T \int d^3r \int d^2u \int d\alpha f(r; u; \alpha): \quad (2)$$

Here  $N$  is the number of rods. We define the surface tension by the difference

$$\sigma = \frac{\Omega_0}{S} = -k_B T \int d^3r \int d^2u \int d\alpha \frac{h}{2} \frac{d}{d\alpha} \ln f(r; u; \alpha) e^{-U_b(r; u; \alpha)}: \quad (3)$$

Here  $\Omega_0$  is the average density of the rods and  $S$  is the surface area of the wall. To compute the integral in Eq. (3), we enumerate all the configurations of the bent rod just touching the walls.

Let us first consider a single flat wall, as shown in Fig. 1. There are three regions to consider: (i)  $0 < \alpha \leq \pi/4$ , (ii)  $\pi/4 < \alpha \leq \pi/3$ , and (iii)  $\pi/3 < \alpha \leq \pi/2$ . For  $\alpha \leq \pi/4$ , we observe that when  $\alpha_1(z; \alpha) < \alpha < \alpha_2(z; \alpha)$ , for

$$\alpha_1(z; \alpha) = \cos^{-1} \frac{h}{2L \cos \alpha} \quad (4)$$

$$\alpha_2(z; \alpha) = \alpha + \cos^{-1} \frac{z}{L}; \quad (5)$$

the rotation of the rod about its symmetry axis is restricted to  $\alpha_a < \alpha < \alpha_b$ , where

$$\alpha_a(z; \alpha) = \cos^{-1} \frac{h}{L \sin \alpha} \quad \alpha_b(z; \alpha) = \alpha + \cos^{-1} \frac{z}{L}: \quad (6)$$

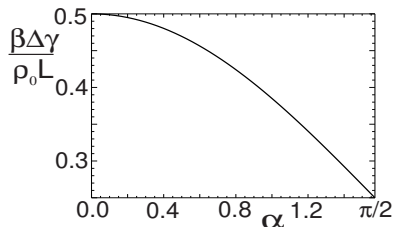


FIG. 2: The surface tension of a bent rod in the presence of a flat plane wall.

Using this construction, the surface tension is

$$\sigma = \frac{\Omega_0}{S} = \frac{L \cos \alpha}{2} + \frac{L}{2} \int_0^{\alpha_1} d\alpha \int_{\alpha_1}^{\alpha_2} d\alpha \sin \alpha f(r; \alpha); \quad (7)$$

where  $x = z/L$ . Similarly, for  $\pi/2 < \alpha < \pi/4$ , we have

$$\sigma = \frac{L \cos \alpha}{2} + \frac{L}{2} \int_0^{\alpha_1} d\alpha \int_{\alpha_1}^{\alpha_2} d\alpha \sin \alpha f(r; \alpha) + \frac{L}{2} \int_{\alpha_1}^{\alpha_2} d\alpha \int_{\alpha_2}^{\alpha_3} d\alpha \sin \alpha f(r; \alpha): \quad (8)$$

In Fig. 2, we plot  $\sigma$  as a function of  $\alpha$ . Note that the limiting values,  $\sigma(0) = \frac{1}{2} k_B T L$  and  $\sigma(\pi/2) = \frac{1}{4} k_B T L$ , agree with previous results [14].

We now turn to the calculation for two walls (see Fig. 1). Since the rods are stiff and  $\alpha$  is small in the experiment of interest, we focus on the case where  $\alpha \leq \pi/4$ . For a given separation of the walls  $d$ , we divide the interval  $0 < z < d/2$  into different regions, wherein  $\alpha_1; \alpha_2; \alpha_3$  and  $\alpha_4$  take on different values. The new angles are

$$\alpha_1(z; \alpha) = \cos^{-1} \frac{d}{2L} \frac{z}{L} \quad (9)$$

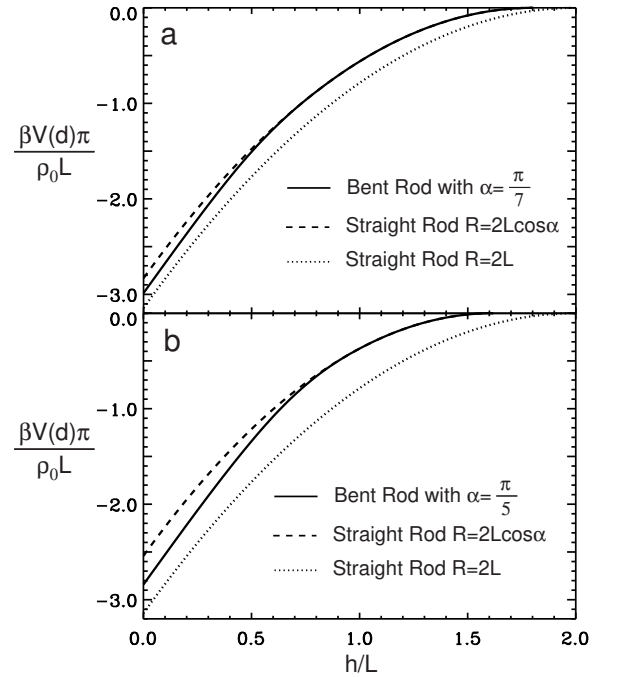


FIG. 3: The depletion interaction  $V(d)$  [Eq. (12)] between two planar walls (the solid curve) mediated by a bent rod of contour length  $L_c = 2L$  with (a)  $\alpha = \pi/7$  and (b)  $\alpha = \pi/5$ . The dashed curve is the depletion interaction of a straight rod with  $R = 2L \cos \alpha$ . At large distances, they show little difference but the restriction on the additional degree of freedom at shorter distances gives rise to a stronger attraction in  $V(d)$ , which is bounded below by the potential of a straight rod of  $R = 2L$  (the dotted line). This is qualitatively the effect observed in experiment of Ref. [10] (See also Fig. 4).

$$\phi_4(z; \theta) = \cos^{-1} \frac{d - z}{2L \cos \theta} : \quad (10)$$

If  $\phi_1 < \phi_2$  and  $\phi_2 < \phi_3$ ,  $\theta$  is restricted to  $\phi_1 < \theta < \phi_3$ . If  $\phi_3 < \phi_4$ ,  $\theta$  is restricted to  $0 < \theta < \phi_4$  and  $\phi_1 < \theta < \phi_2$  with

$$\phi_b(z; \theta) = \cos^{-1} \left( 1 - \frac{L \cos(\theta - \phi_1)}{L \sin \phi_1 \sin(\phi_2 - \phi_1)} \right) \frac{(d - z)}{2L \cos \theta} : \quad (11)$$

When  $\phi_2 > \phi_3$ ,  $\theta$  is further restricted to  $\phi_1 < \theta < \phi_2$  and  $\phi_3 < \theta < \phi_4$  if  $\phi_3 < \phi_2$ . Thus, the depletion potential per unit area defined by  $V(d) = \int_{\phi_1}^{\phi_2} \int_{\phi_3}^{\phi_4} \phi(z; \theta) d\theta dz$  is

$$V(d) = \frac{1}{2} k_B T L \cos \theta \left( 1 - \frac{d}{2L \cos \theta} \right)^2 + \int_{\phi_1}^{\phi_2} \int_{\phi_3}^{\phi_4} \phi(z; \theta) dz d\theta ; \quad (12)$$

where

$$\phi(z; \theta) = \frac{1}{2} \int_{\phi_1}^{\phi_2} \int_{\phi_3}^{\phi_4} dz d\theta \sin \theta \phi_a(z; \theta) + \frac{1}{2} \int_{\phi_1}^{\phi_2} \int_{\phi_3}^{\phi_4} dz d\theta \sin \theta \phi_b(z; \theta) : \quad (13)$$

Here  $\int$  indicates integrations over phase space restricted to the allowed values. Fig. 3 depicts the depletion potential between two walls for different  $\theta$ . At large distances the potential is determined by the "end-to-end" distance  $R$  of the rod. At short distances the rotational degree of freedom becomes important and increases the attraction

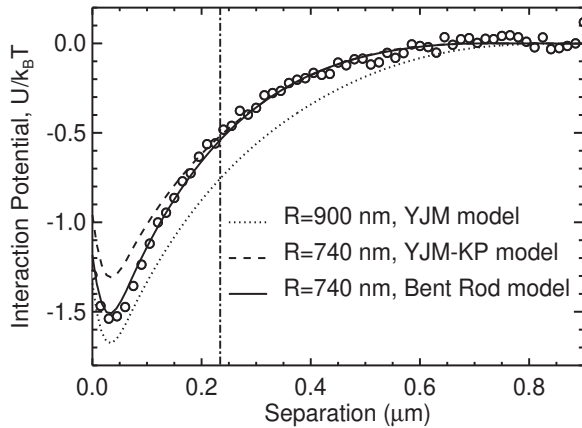


FIG. 4: Interaction potential between a pair of 1.0  $\mu\text{m}$  silica spheres in a suspension of fd virus with concentration 0.67 mg/ml. The dotted (dashed) lines are generated by the YJM model with  $R = L_c = 900$  nm ( $R = 740$  nm;  $L_c = 900$  nm). The solid lines are generated by Eq. (14) with  $R = 740$  nm and  $L_c = 900$  nm. Clearly, the agreement of experimental data and our model which includes the additional rotational degree of freedom of a bent rod is excellent. The dash-dotted vertical line indicates  $W = 0.23$   $\mu\text{m}$ .

between walls. The potential is bounded below by the potential of a straight rod with length  $2L$ . Although our calculation has been done for two walls, we expect the same qualitative features to hold for two spheres.

$V(d)$  can be written as a sum of 2 pieces. The first term is the depletion potential of a straight rod with length  $R = 2L \cos \theta$  [14]. The second term depends only on the additional rotational degree of freedom of the bent rod. Moreover, the range of  $(d; \theta)$  is of order of the width of the bent rod,  $W = L \sin \theta$ , which is small compared to the sphere radius in Ref. [10]. These observations suggest that to approximate the depletion potential for two spheres, the latter term may be treated in the Derjaguin approximation, while the first term replaced by the YJM rigid-rod model [5]. Thus, we write

$$U_s(h) = \frac{1}{2} a R^2 K \left( \frac{h}{R}; \frac{a}{R} \right) + \frac{1}{R^2} \int_{\phi_1}^{\phi_2} dx \phi(x; \theta) ; \quad (14)$$

where  $a$  is the sphere radius and  $h$  their closest surface separation.  $K(h=R; a=R)$  is the potential between two spheres due to a straight rod of length  $R$ , which reduces to the Derjaguin expression  $K_D(h=R) = \frac{1}{6} (1 - h/R)^3$  in the limit  $a=R$  [5].

Fig. 4 displays a typical experimental data set of Ref. [10] with three different models: (i) the YJM model (dotted line), whose potential is given by the first term

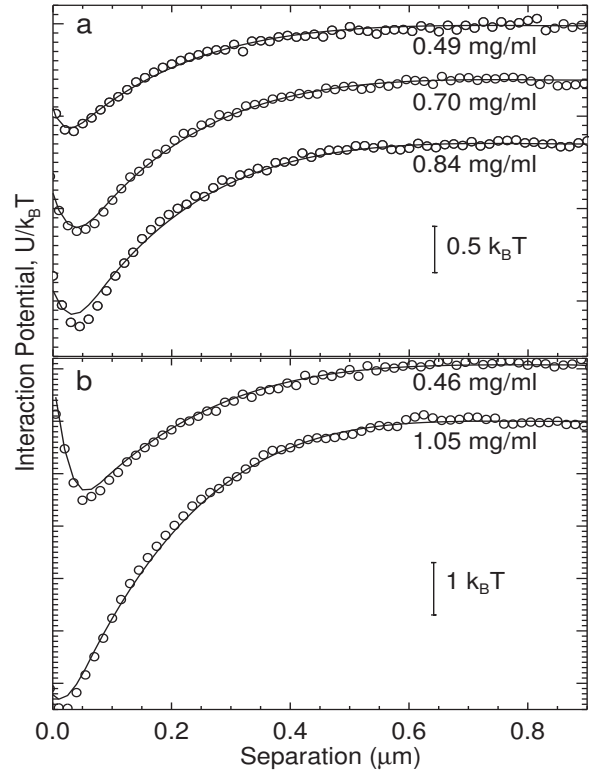


FIG. 5: Interaction potential between pairs of (a) 1.0  $\mu\text{m}$  and (b) 1.6  $\mu\text{m}$  silica spheres in a suspension of fd virus with different concentration. The solid lines are generated by Eq. (14), with best fit parameters that give smallest  $\chi^2$ .

in Eq. (14) with  $R = 900$  nm, the contour length of fd, (ii) the YJM-KP model (dashed line), whose potential is given by the first term in Eq. (14) with  $R = 740$  nm, and (iii) the bent rod model (solid line),  $U_s(h)$  in Eq. (14) with  $R = 740$  nm and  $L_c = 900$  nm. The circles are experimental data for 1.0  $\mu$ m diameter silica particle in a dilute (0.67 mg/ml) solution of fd virus. The theory curves are computed with no free parameters and are then numerically blurred to account for the instrument's spatial resolution (see Ref. [10]). Clearly, our model gives the best fit to the experimental data. In particular, both YJM and YJM-KP models, while having approximately the right magnitude and shape, fail to account for the overall curvatures of the experimental curve. Further, while the YJM-KP model agrees with most of the data at large  $h$ , our model clearly accounts for the depth of the measured potential near contact.

In order to explore the best fits more quantitatively, we computed the  $\chi^2$  value of our models for all data sets with  $R$  ranging from 720–825 nm and  $L_c = 880, 900$ , and 920 nm. If a fixed concentration (measured experimentally) is assumed,  $\chi^2$  is smallest for  $R = 780$  nm and  $L_c = 920$  nm. If the concentration is allowed to vary within its 5% experimental error, then  $\chi^2$  is smallest for  $R = 740$  nm and  $L_c = 900$  nm. Fig. 5 shows best fits for each of concentration. Note that the width  $W = 200$  nm, is smaller than the radius of the colloidal spheres. This justifies a posteriori the Derjaguin approximation made in Eq. (14). Furthermore, we can estimate  $\lambda_p$  using Eq. (1) and the values for  $R$  and  $L_c$  above, yield-

ing  $\lambda_p \approx 850$  nm (fixed concentration) and  $\lambda_p \approx 680$  nm (variable concentration). Our results for  $L_c$  of fd are consistent with the literature, i.e.  $850 \text{ nm} < L_c < 920 \text{ nm}$  [15]. However, our values for  $\lambda_p$  should be contrasted to the often-quoted value,  $\lambda_p = 2.2 \mu\text{m}$  [16, 17]. The latter is based on a fitting of dynamic light scattering data with theoretical models [17, 18], whose assumptions may well be questioned in the light of our results. Indeed, smaller values of  $\lambda_p$  have also been reported based on dynamic structure factor models of semi-flexible lamellae [19], and using electron microscopy [20].

We have presented a simple analytical model for the depletion interaction between two spheres mediated by semi-flexible rods, and demonstrated its quantitative agreement with experimental data. Our theoretical model combined with interaction measurements provides a basis for extracting the persistence length of a semi-flexible rod.

#### Acknowledgments

We thank R.D. Kamien, Tom Lubensky, C.M. Marques, and Fylypus for valuable discussions. A.W.C.L. is particularly grateful to K. Yamamoto for sharing his insights. This work is supported by the NIH Grant HL67286, and partially supported by the NSF through DMR-0203378 and the MRSEC Grant DMR-00-79909.

- 
- [1] W.B. Russel, D.A. Saville, and W.R. Schowalter, *Colloidal Dispersions* (Cambridge University Press, Cambridge, 1989)
  - [2] M. Adams, Z. Dogic, S.L. Keller, and S. Fraden, *Nature* (London) 393, 349 (1998).
  - [3] G.H. Koenderink et al., *Langmuir* 15, 4693 (1999); G.A. Vliegenthart, A. van Blaaderen, and H.N.W. Lekkerkerker, *Faraday Discuss.* 112, 173 (1999).
  - [4] S.M. Ilett, A. Orock, W.C.K. Poon, and P.N. Pusey, *Phys. Rev. E* 51, 1344 (1995).
  - [5] K. Yamamoto, C. Jeppesen, and C.M. Marques, *Europhys. Lett.* 42, 221 (1998).
  - [6] Y. Ma, M.E. Cates, and H.N.W. Lekkerkerker, *Phys. Rev. Lett.* 75, 4548 (1995).
  - [7] M. Piech and J.Y. Walz, *J. Colloid Interface Sci.* 232, 86 (2000); F. Schlesener, A. Hanke, R. Kimpel, and S. Dietrich, *Phys. Rev. E* 63, 041803 (2001).
  - [8] P. van der Schoot, *J. Chem. Phys.* 20, 9132 (2000).
  - [9] M. Triantafyllou and R.D. Kamien, *Phys. Rev. E* 59, 5621 (1999).
  - [10] Keng-Hui Lin, John C. Crocker, Ana C. Zeri, and A.G. Yodanis, *Phys. Rev. Lett.* 87, 088301 (2001); the mean end-to-end distance  $R$  of the fd-virus was incorrectly computed in this paper to be  $R = 780$  nm using  $\lambda_p = 2.2 \mu\text{m}$ . It should have been  $R = 825$  nm.
  - [11] S. Asakura and F. Osawa, *J. Chem. Phys.* 22, 1255 (1954); *J. Polym. Sci.* 33, 183 (1958).
  - [12] The reported values of the persistence length of fd are either measured by electron microscopy (EM) or dynamic light scattering (DLS). While the reported value from EM varies from  $\lambda_p = 0.98$  to  $6.6 \mu\text{m}$  [see K. Beck and R.M. Duenki, *J. Struct. Bio.* 105 22 (1990)], DLS gives  $\lambda_p = 2.2 \mu\text{m}$  (see Refs. [16, 17]).
  - [13] M. Doi and S.F. Edwards, *The Theory of Polymer Dynamics* (Oxford University Press, Oxford, 1986)
  - [14] K. Yamamoto, M. Jeng, P. Pincus, C. Jeppesen, and C.M. Marques, *Physica A* 247, 159 (1997).
  - [15] L.A. Day, C.J. Marzec, S.A. Reisberg, and A. Casadevall, *Ann. Rev. Biophys. Chem.* 17, 509 (1988).
  - [16] E. Loh, E. Ralston, and V.N. Schumaker, *Biopolymers* 18, 2549 (1979); T. Maeda and S. Fujime, *Macromolecules* 18, 2430 (1985).
  - [17] L. Song, U. Kim, J.W. Ilcoxon, and M. Schurr, *Biopolymers* 31, 547 (1991).
  - [18] K. Roy and E. Frey, *Phys. Rev. E* 55, 3092 (1997); T.B. Liverpool and A.C. Maggs, *Macromolecules* 34, 6064 (2001).
  - [19] Andreas Augustin, Masters thesis, Technischen Universität München (1999), pp 61.
  - [20] J. Tang, Ph.D. thesis, Brandeis University (1995), pp 12.